

DESIGN STUDIES FOR MEDIUM AND HIGH BETA SCRF CAVITIES FOR INDIAN SPALLATION NEUTRON SOURCE*

Arup Ratan Jana and Vinit Kumar[#]

Materials and Advanced Accelerator Sciences Division
RRCAT, Indore 452013, India

Abstract

There is a plan to build a 1 GeV H⁺ linac for the proposed Indian Spallation Neutron Source (ISNS) at Raja Ramanna Centre for Advanced Technology (RRCAT), Indore. The medium and high energy section of the ISNS linac will consist of $\beta_g = 0.61$, as well as $\beta_g = 0.9$, 650 MHz, 5-cell superconducting radiofrequency (SCRF) cavities, for which detailed design studies have been performed. During our design study, we have evolved a generalized procedure for the optimization of geometrical parameters of multi-cell elliptic SCRF cavities. Studies on higher order modes supported by the cavity, and its effect on beam dynamics, as well as on cryogenic heat load have been performed. Finally, studies have been performed to minimize the effect of Lorentz Force Detuning (LFD). The paper discussed these calculations and initial beam dynamics studies.

geometric beta (β_g) of cavities, we have opted for two families of SCRF cavities: 5-cell, $\beta_g = 0.61$ cavities to accelerate the particles from 150 MeV to 500 MeV, followed by 5-cell, $\beta_g = 0.9$ cavities to further accelerate the particles to 1 GeV. In the next section, we describe the electromagnetic design of SCRF cavities. This is followed by discussion of Lorentz Force Detuning (LFD) studies and initial results of beam dynamics studies.

ELECTROMAGNETIC DESIGN STUDIES

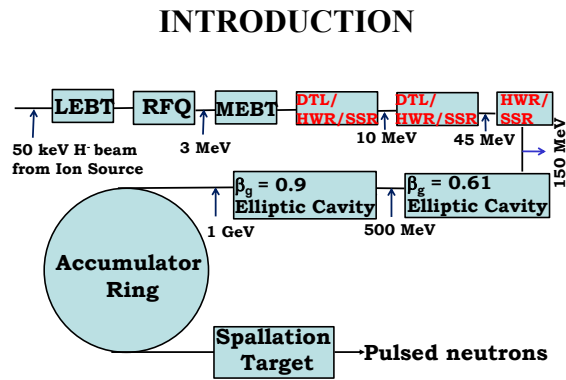


Figure 1: A schematic of the accelerator for ISNS.

It is proposed to build a spallation neutron source at Raja Ramanna Centre for Advanced Technology (RRCAT) in India for experimental studies of condensed matter physics and various engineering applications [1]. A schematic configuration of the injector linac and the accumulator ring that will produce $\sim 1 \mu\text{s}$ pulses of 1 GeV proton beam is shown in Fig. 1. Physics design studies of various accelerators and beam transport lines have commenced at RRCAT. In this paper, we describe our recent design studies of Superconducting Radiofrequency (SCRF) cavities. Operating frequency of the SCRF cavities is chosen as 650 MHz in order to utilize the indigenously developed solid state RF power sources at this frequency. Based on the calculations of transit time factor in the operating range of beam energies, for different values of

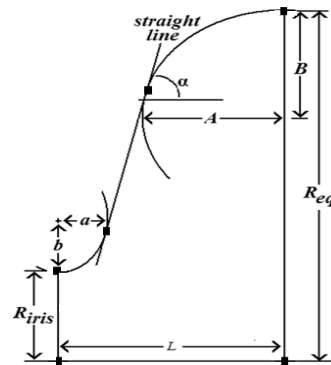


Figure 2: Schematic of the half-cell of an elliptic cavity.

We first discuss the optimization of the geometrical parameters of an SCRF cavity. Figure 2 shows the cross section of the half-cell, which is obtained by joining two elliptical arcs by a common tangent, and is described by seven parameters – iris ellipse radii a and b , equator ellipse radii A and B , iris radius R_{iris} , equator radius R_{eq} , and half-cell Length L . Since the cavity operates in π mode, $L = \beta_g \lambda / 4$, where λ is the free space wavelength corresponding to the operating RF frequency. Choice of R_{iris} is made to ensure that it is just enough to provide the required cell-to-cell coupling, while not affecting the shunt impedance significantly. The maximum feasible value is chosen for the cavity wall angle α since it results in reduced heat loss on the cavity wall. In our design, these values are 85° and 88° for $\beta_g = 0.9$ and 0.61 cavities respectively. The required resonant frequency is achieved by tuning R_{eq} . The remaining three independent geometrical parameters are optimized to minimize the value of E_{pk}/E_{acc} and B_{pk}/E_{acc} , where E_{pk} and B_{pk} are the peak electric and magnetic fields respectively on the cavity surface, and E_{acc} is the average acceleration gradient in the cavity. In our generalized design procedure, we first put the constraint $a/b = A/B = 1$, and plot E_{pk}/E_{acc} and B_{pk}/E_{acc} as a function of B , as shown in Fig. 3, using the computer code SUPERFISH [2]. The

*Work supported by Department of Atomic Energy, Govt. of India
[#]vinit@rrcat.gov.in

optimum value of B is chosen, where E_{pk}/E_{acc} just starts increasing rapidly, to ensure that both E_{pk}/E_{acc} and B_{pk}/E_{acc} are minimized. The remaining two independent geometrical parameters, a/b and A are then tuned to minimize B_{pk}/E_{acc} , keeping a fixed target value of E_{pk}/E_{acc} . Based on this generalized procedure [3,4], the optimized value of geometrical parameters of the mid-cells were obtained, which are shown in Table 1 and 2 for $\beta_g = 0.9$ and 0.61 respectively. Beam pipe radius is same as R_{iris} .

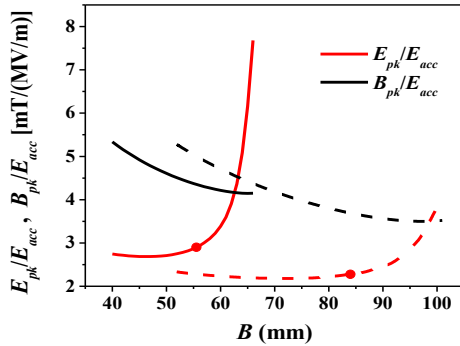


Figure 3: Variation of B_{pk}/E_{acc} and E_{pk}/E_{acc} with B for $\beta_g = 0.61$ (solid curve), and 0.91 cavity (dashed curve).

Table 1: Optimized Parameters of $\beta_g=0.9$ Cavity

Geometry parameters	Mid-cell	End-cell
R_{iris} (mm)	50.00	50.00
R_{eq} (mm)	199.925	199.925
L (mm)	103.774	105.800
A (mm)	83.275	83.275
B (mm)	84.00	84.00
a (mm)	16.79	16.79
b (mm)	29.45	29.45

Table 2: Optimized Parameters of $\beta_g=0.61$ Cavity

Geometry parameters	Mid-cell	End-cell (entry)	End-cell (exit)
R_{iris} (mm)	44.00	44.00	44.00
R_{eq} (mm)	195.591	195.591	195.591
L (mm)	70.336	71.550	71.240
A (mm)	52.64	52.64	52.25
B (mm)	55.55	55.55	55.55
a (mm)	15.28	15.28	15.28
b (mm)	28.83	28.83	28.83

End-cell parameters are same as the mid-cell parameters, except that there is slight tuning in the values of L and A . For $\beta_g = 0.9$ cavities, it was sufficient to tune the value of L alone such that the value of resonant frequency of $TM_{010} - \pi$ mode for the full cavity with end-cells including the beam pipe is same as that of the mid-cell with appropriate

boundary conditions. This ensures that there is good field flatness in the cavity. For $\beta_g = 0.9$ cavity, there was no trapped higher order mode with frequency less than the cut-off frequency of the beam pipe. However, for $\beta_g = 0.61$ cavity, there was a trapped monopole mode at 1653.20 MHz. Hence, in order to take care of the trapped mode, in addition to L , we need to tune A for the end cell at the exit end, as shown in Table 2. HOM studies have been performed using the computer codes SLANS [5]. A detailed calculation of threshold current for the regenerative beam break up instability due to dipole modes was performed for these cavities. In the absence of HOM couplers, the CW average of threshold currents were calculated as 0.85 mA and 0.7 mA respectively for $\beta_g = 0.9$ and 0.61 cavities, which are acceptable. With the help of HOM couplers, it should be easily possible to operate at CW average current of 1 mA.

Calculations of heat load resulting due to a possible scenario that HOM frequency is integral multiple of frequency of any of the Fourier components of beam current has also been done in detail, following the approach described in Ref. [6]. We have shown that for our beam pulse structure, the cryogenic load due to HOMs will not be very significant if we keep the external quality factor Q_{ext} for HOMs less than 10^8 [4].

LORENTZ FORCE DETUNING STUDIES

For SCRF cavities, one important issue that needs to be addressed is the LFD, which arises due to pressure of the RF field on the cavity wall. This is important due to high value of Q_{ext} of the cavity for the operating mode, which reduces the cavity bandwidth. In our case, we expect the operating value of Q_{ext} around 5×10^6 , which gives a cavity bandwidth of 120 Hz. If the LFD is more than this value, the cavity needs to be tuned back using fast tuners. We have performed a detailed analysis of LFD for which subroutines have been written in ANSYS [7] parametric design language to perform coupled electromagnetic and structural analysis. Figure 4 shows the schematic of the cavity with helium vessel and stiffener rings, which are used to increase the stiffness of the cavity to reduce the cavity detuning. Helium vessel will be made of titanium, and it will be joined with cavity using a transition piece made of 55Ti-45Nb alloy.

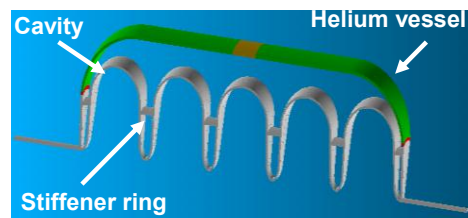


Figure 4: Schematic of the cavity with the helium vessel.

In our analysis, we have optimized the following parameters: cavity wall thickness, helium vessel thickness, shape of the end closure of the helium vessel and location

of stiffener rings. Optimization is done to ensure that for the operating gradients (18.6 MV/m for $\beta_g = 0.9$ cavity, and 15.4 MV/m for $\beta_g = 0.61$ cavity), the LFD is within the value that can be compensated with a tuner. Also, for the pulsed operation, we have ensured that none of the prominent Fourier components of the RF pressure pulse are close to the structural mode frequencies [4,8]. Based on our analysis, we have obtained the cavity wall thickness as 4 mm, the helium vessel thickness as 5 mm, and the radial location of the stiffener ring as 124 mm for the $\beta_g = 0.61$ cavity, and 119.5 mm for the $\beta_g = 0.9$ cavity. Diameter of helium vessel is chosen as 504 mm, with end closure in “tori-spherical” shape with torus radius of 120 mm.

BEAM DYNAMICS STUDIES

We now discuss the beam dynamics studies to find out a suitable lattice consisting of cavities, drift spaces and focusing quadrupole doublets to accelerate and focus the 150 MeV beam to 1 GeV. Pulse beam current is taken as 15 mA in our calculations. The normalized rms beam emittance is taken as 0.25 mm-mrad in the transverse direction, and 0.16 mm-mrad in the longitudinal direction. We have used beam dynamics codes GENLINWIN and TRACEWIN [9] for our analysis. Basic criterion has been to optimize the lattice such that there is good beam transmission without invoking any beam instability. We have used the following guiding recipes for the choice of suitable lattice – (i) zero current phase advance per focusing period in all planes should be less than 90 degree in order to avoid envelope instability, (ii) phase advance per unit length should change adiabatically along the linac, to ensure current independent matching (iii) strong space charge resonance in Hoffmann diagram should be avoided, and tune depression should be > 0.5 to ensure that effect of space charge is not detrimental, and (v) beam pipe radius / rms beam size > 10 to ensure that there is no beam loss.

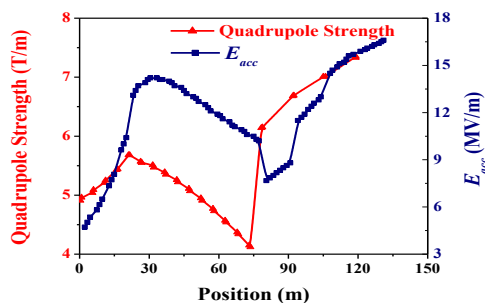


Figure 5: Quadrupole gradient and E_{acc} along the linac.

For the $\beta_g = 0.61$ section, we have chosen the lattice period configuration as FDRRR, where FD and R denote the quadrupole doublet and cavity resonator respectively. There will be fifteen periods, and each period will be 5.2 m long. This will be followed by $\beta_g = 0.9$ section with four periods, and each period will be 13.56 m long with FDRRRRRRRR configuration. Figure 5 shows the quadrupole strengths and E_{acc} in cavities along the length

of the linac. Variation of rms beam size is shown in Fig.6. It has been checked that the criteria mentioned in the last paragraph are satisfied. It is seen from Fig. 7, that there is no danger of strong space charge resonance.

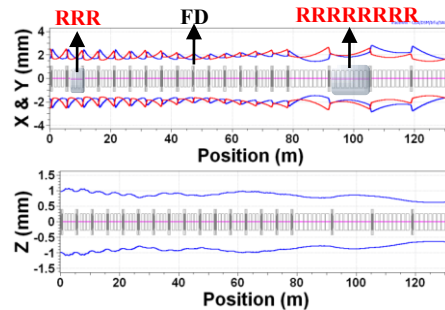


Figure 6: Variation of rms beam size along the linac.

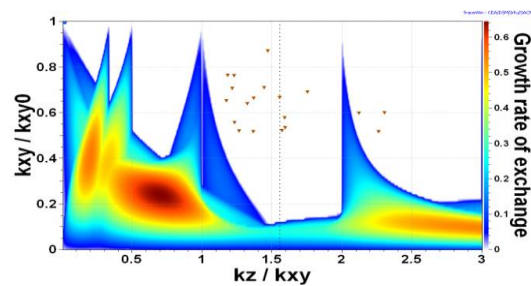


Figure 7: Hoffmann diagram for the lattice.

To summarize, we have presented the electromagnetic design and first order beam dynamics studies of medium and high beta section of the 1 GeV injector linac for the proposed ISNS project. Design criteria and the methodology adopted have been elaborated. Further studies on the effect of failure of some of the lattice elements on the beam dynamics will be taken up.

It is a pleasure to thank Mr. Abhay Kumar for helpful discussions on LFD. We would like to thank Dr. S. B. Roy and Dr. P. D. Gupta for constant encouragement.

REFERENCES

- [1] V. Kumar, A. Sharma and S. B. Roy, Indian Nuclear Society News **10**, 60 (2013).
- [2] K. Halbach et al., Particle Accelerators **7** 213 (1976).
- [3] A. R. Jana et al., IEEE Trans. Applied Superconductivity **23**, 3500816 (2013).
- [4] A. R. Jana and V. Kumar, IEEE Trans. Applied Superconductivity (accepted for publication).
- [5] D. Myakishev and V. Yakovlev, Proceedings of PAC 2348 (1995).
- [6] S. H. Kim and M. Doleans, Nucl. Instr. and Meth. A **492** 1 (2002).
- [7] ANSYS Theory Reference, <http://www.ansys.com>
- [8] A. Kumar, A. R. Jana and V. Kumar, Nucl. Instr. and Meth. A **750** 69 (2014).
- [9] D. Uriot, <http://irfu.cea.fr/Sacm/logiciels/index3.php>